Available online at www.sciencedirect.com
SCIENCE DIRECT®
Journal of Chromatography A, 1089 (2005) 72–81
JOURNAL OF CHROMATOGRAPHY A
www.elsevier.com/locate/chroma

Assessment of supporting electrolyte contributions in electrochemically modulated liquid chromatography

David W. Keller, Lisa M. Ponton [1], Marc D. Porter *

Ames Laboratory, USDOE, Institute for Combinatorial Discovery, and Department of Chemistry, Iowa State University, Ames, IA 50111, USA

Received 10 March 2005; received in revised form 7 June 2005; accepted 14 June 2005
Available online 15 July 2005

Abstract

This paper reports the results of an investigation on the role of the supporting electrolyte in separations using electrochemically modulated liquid chromatography (EMLC) with a porous graphitic carbon stationary phase. With respect to the identity of the supporting electrolyte, the elution strength of the electrolyte anion increased as $F^- < OH^- < BF_4^- < ClO_4^- < PF_6^-$ for injections of negatively charged aromatic molecules, whereas a 10-fold increase in electrolyte concentration induced a 60% change in retention for the same solutes. Furthermore, both the concentration and composition of the supporting electrolyte affected retention in a manner that varied with the charge of the analyte and applied potential. This behavior is explained using Gouy–Chapman diffuse double layer theory, coupled with comparisons of this theory with closely related models for ion-pair chromatography. Insights into the retention mechanism reveal that an ion-exchange mechanism controls the retention of negatively charged solutes at applied potentials removed from the potential of zero charge (PZC). At potentials close to the PZC, the electrostatic model is less effective with the predominant retention mechanism likely involving hydrophobic interactions with the carbonaceous stationary phase. The combined effects of these findings are demonstrated by using a temporal gradient in supporting electrolyte concentration to optimize an EMLC separation.

Keywords: Electrochemically modulated liquid chromatography; Ion exchange chromatography; Electrical double layer theory; Porous graphite carbon

1. Introduction

Electrochemically modulated liquid chromatography (EMLC) is a unique union of electrochemistry and chromatography [1,2]. This union is accomplished by using a conductive stationary phase (e.g., porous graphitic carbon, PGC) as the working electrode in a three-electrode electrochemical cell that is also configured as the stationary phase of a LC column. Changes in the potential applied (E_{app}) to the stationary phase can therefore manipulate the efficiency of a separation in a manner likened to that of mobile phase gradients in LC. EMLC has been applied to a wide range of separations, including mixtures of aromatic sulfonates [3–5], monosubstituted benzenes [6], dansylated amino acids [7], corticosteroids [8,9], benzodiazepines [9,10], the enantiomers of hexabarbital and mephenytoin [11], short chain alkanoic acids [12], and metal ion complexes [13]. Moreover, operation at elevated temperatures has been used to complete EMLC separations with marked reductions in elution time [14].

EMLC differs from conventional LC because the effective composition of the stationary phase can be controlled. To do so, however, requires the presence of a supporting electrolyte in the mobile phase. In electrochemistry, the supporting electrolyte performs three key functions; it: (1) increases solution conductivity; (2) minimizes migration effects; and (3) creates a reproducible electrical double layer [15]. In addition to serving the same purposes in EMLC, the supporting electrolyte may have an impact on a separation through interactions with the analyte or by competition for sorption on the stationary phase. This paper is the first in a series of investigations

* Corresponding author. Tel.: +1 515 294 6433; fax: +1 515 294 6433.
E-mail address: mporter@porter1.ameslab.gov (M.D. Porter).
[1] Present address: Chemistry Department, Elon University, Elon, NC 27244, USA.

0021-9673/$ – see front matter © 2005 Elsevier B.V. All rights reserved.
doi:10.1016/j.chroma.2005.06.082

aimed at delineating the role of supporting electrolyte in EMLC, and ultimately, the retention mechanism in EMLC.

In EMLC, the influence of E_{app} on retention is often summarized by changes in the retention factor (k'). A plot of log k' versus E_{app} (i.e., a capacity–potential curve) is linear when the retention is dominated by electrostatic interactions, behavior that follows a Boltzmann distribution of ions in an electric field [7,16]. This dependence is common for small ions, including many aromatic sulfonates. However, other analytes exhibit nonlinear capacity–potential curves, including several uncharged molecules and, to a lesser extent, some charged analytes. These examples show that the pure electrostatics model must be refined [17]. The work herein is therefore aimed at extensions of the electrostatic model by using Gouy–Chapman diffuse double layer theory in an attempt to account for competition for adsorption sites between the supporting electrolyte and analyte as a function of E_{app}.

Fig. 1 illustrates several of the thermodynamic pathways in which the supporting electrolyte may influence retention. It shows the competition between supporting electrolyte and analyte for adsorption sites on the stationary phase as well as interactions between an electrolyte ion and analyte both on the stationary phase and in the mobile phase. Thus, the free energy of adsorption for an analyte (ΔG_{tot}) is a combination of the free energies of interactions between all species in the system, which is manifested in the retention of the analyte.

The interactions that occur directly between the analyte and the stationary phase are defined as $\Delta G_{a\text{-lyte}}$ and include, for example, hydrophobic and donor–acceptor interactions. The free energy for adsorption of supporting electrolyte is defined by $\Delta G_{\pm e\text{-lyte}}$. This term can be split into electrolyte cations, $\Delta G_{+e\text{-lyte}}$, and electrolyte anions, $\Delta G_{-e\text{-lyte}}$. The free energy of interaction between an analyte and surface-bound supporting electrolyte is given by $\Delta G_{+N\text{-}N}$ for cations and $\Delta G_{-N\text{-}N}$ for anions, noting that these interactions differ from those in bulk solution (ΔG_{+int} for cations or ΔG_{-int} for anions).

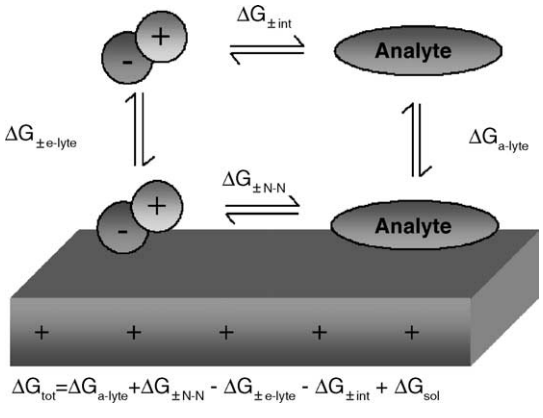

Fig. 1. Thermodynamic interactions describing the influence of supporting electrolyte on adsorption onto the stationary phase in an EMLC experiment (see text for details).

For simplicity, Fig. 1 neglects the possible presence of oxygen-containing functional groups on the carbon surface and omits the role of mobile phase solvent, ΔG_{sol}. The effect of oxygen containing functional groups on retention on PGC stationary phases warrants further study [13,18–20]. On the other hand, the role of solvent and organic modifiers on retention has been studied extensively for PGC in conventional HPLC settings [21–26]. Temperature studies in EMLC have recently shown that changes in retention as a function of E_{app} are entropically driven [27]. Taken together, the complexity of the possible contributions to retention in EMLC point to the need to determine the factors that dominate system behavior.

This paper advances insights into the retention mechanism by assessments of the role of supporting electrolyte. We have therefore monitored changes in retention for small aromatic ions by systematically varying the concentration and composition of the electrolyte. To facilitate this analysis, the Gouy–Chapman (G–C) double layer theory is adapted for use with the chromatographic data from EMLC. This development is then compared to models for ion-pair chromatography [28–31]. Lastly, the combined effects of these findings are exploited by using a temporal gradient in supporting electrolyte concentration to optimize an EMLC separation.

2. Experimental

2.1. Chemicals

With the exception of *p*-hydroxybenzenesulfonate (see below), all test analytes used herein are electroinactive over the experimentally tested range of E_{app} [7,16]. Sodium benzenesulfonate (BS), sodium *p*-toluenesulfonate (TS), pyridine (PYR), disodium 1,3-benzenedisulfonate (BDS), sodium *p*-hydroxybenzenesulfonate (HBS), trifluoroacetic acid (TFA), dibromomethane, and lithium perchlorate were purchased from Aldrich (Milwaukee, WI, USA). Sodium *p*-chlorobenzenesulfonate (CBS) was obtained from TCI America (Portland, OR, USA). *N*-Methylaniline (NMA) and disodium 1,5-naphthalenedisulfonate (1,5-NDS) were acquired from Eastman Kodak (Rochester, NY, USA). Acetonitrile and sodium fluoride were purchased from Fisher Scientific (Fair Lawn, NJ, USA). All chemicals were used as received. Distilled water was further purified with a Millipore Milli-Q system (Bedford, MA, USA). Before use, the solutions were filtered through a 0.5 μm filter (GE Osmonics, Minnetonka, MN, USA), and thoroughly sparged with helium.

2.2. EMLC columns

The construction of the column is described in detail elsewhere [3]. In short, these columns consist of a Nafion cation-exchange membrane in tubular form (Perma Pure, Toms River, NJ, USA) that is inserted into a porous stainless steel cylinder (Mott Metallurgical, Farmington, CT, USA).

The column is slurry packed with PGC (ThermoHypersil, Bellefonte, PA, USA), which serves as a working electrode and stationary phase. The porous stainless steel cylinder prevents deformation of the Nafion tubing under the high pressure of chromatographic flow and is also used as the auxiliary electrode. The Nafion tubing acts as a container for the stationary and mobile phases, an electron insulator to prevent short-circuits between the auxiliary and the working electrode, and a salt bridge between the internal mobile phase and an external electrolyte reservoir. The external electrolyte reservoir houses a Ag/AgCl saturated NaCl electrode, and all values of E_{app} are reported with respect to this electrode.

The experiments used 5 μm diameter PGC particles as the packing. X-ray photoelectron spectroscopy has shown that PGC is devoid of detectable oxygen-containing surface groups (detection limit: ∼0.2 at.%) [5]. The manufacturer places the nominal pore diameter at ∼250 Å, which yields a porosity of ∼80% [32]. The surface area of the PGC stationary phase is, ca. 30 m^2, based on BET adsorption measurements (120 m^2/g)[33] and the amount packed into the column (∼0.25 g).

2.3. Instrumentation

Chromatographic experiments used a HP 1050 series module HPLC, a quaternary pumping system and a diode array detector (Hewlett-Packard, Santa Clara, CA, USA). Samples were injected via a Rheodyne Model 7125 injector with a 5 μL sample loop (Cotati, CA, USA). The potential of the working electrode/chromatographic packing was controlled with an AMEL Instruments Model 2055 High-Power Potentiostat (Milan, Italy) or a Model 174A Polarographic Analyzer (Princeton Applied Research, Princeton, NJ, USA). The pH of the aqueous phases before mixing with acetonitrile was determined using an Orion model 520 A pH meter (Beverly, MA, USA).

2.4. Mode of operation

To examine the role of supporting electrolyte concentration on retention, the mobile phase composition was manipulated by on-line mixing. Trifluoroacetic acid (TFA) was added to all the salt solutions and water in proportions to set the pH at ∼3 for sample mixtures that contained pyridine (pK_a = 5.24) or *N*-methyl aniline (pK_a = 5.23) [34]; this pH ensures that both analytes are present as monovalent cations in the mixed solvent mobile phase.

When the composition of the mobile phase was changed, the system was allowed to reach a steady state under the new conditions by the longer of two scenarios: the detector baseline became stable or 30 min after the change in conditions. Analyte absorbance was monitored at 220 nm unless noted. Individual injections of each analyte were performed for peak identification, and a water blank was used to determine the solvent front for calculations of k'. The retention times for k' were determined from the first statistical moment [35–37] of the elution band to compensate for tailing.

3. Results and discussion

3.1. Effect of applied potential

The influence of E_{app} on the retention of aromatic sulfonates has previously been demonstrated [3–5]. In short, E_{app} induced changes in retention are consistent with expections based on electrostatic interactions, but vary slightly between solutes and can cause changes in elution order. The modulation of the retention for all eight compounds is summarized in Fig. 2 by plots of ln k' versus E_{app}. The error bars for ln k' are roughly the size of the data symbols and characterize the precision for five replicate injections. With the exception of HBS, each compound follows the linear dependence predicted by the influence of an electric field on a Boltzmann distribution of ions [38].

The correlation coefficients for the plots in Fig. 2 are given in Table 1, and support the linear relationship of ln k' versus E_{app}. However, the break for HBS (Fig. 2, inset) suggests anomalous behavior, which is attributed to the oxidation of the hydroxyl functional group to a carbonyl group [3,39]. The linearity on either side of this break connotes that both compounds maintain an overall negative charge. However, the offset and change in slope indicate that a non-electrostatic component of retention (i.e., hydrophobicity) differs for the two forms. The change in the UV–vis spectrum of the

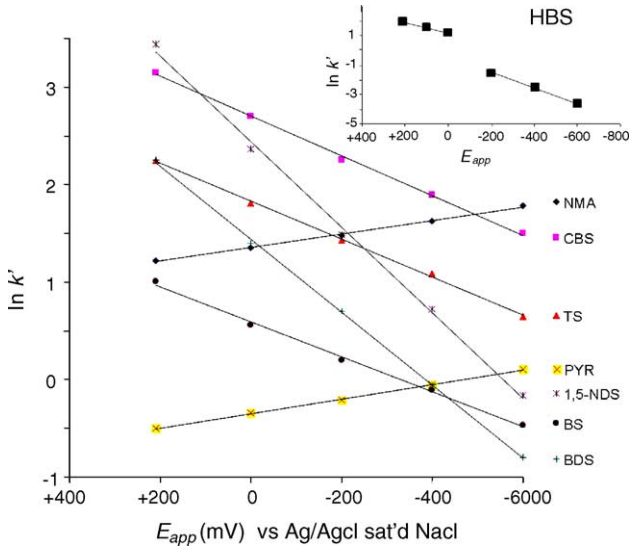

Fig. 2. Plots of ln k' vs. E_{app} for the analytes used in this study. The data points are approximately the size of the error bars from five replicate injections at each E_{app}. The mobile phase was composed of 10% acetonitrile in water for BS (10 μM), TS (18 μM), CBS (23 μM) and 1,5-NDS (26 μM); 5% acetonitrile in water with trifluoroacetic acid added to adjust the pH ∼ 3 for BDS (13 μM), PYR (31 μM) and NMA (22 μM). Lithium perchlorate (0.1 M) was used as the supporting electrolyte at a flow rate of 0.4 mL/min.

Table 1
$\ln k'$ vs. E_{app} for seven of the test analytes

Compound	Ionic charge	Slope[a] of $\ln k'$ vs.	
		E_{app}	R^2
1,5-NDS	−2	−0.0044 ± 00002	0.9973
BDS	−2	−0.0037 ± 00005	0.9986
CBS	−1	−0.0020 ± 00003	0.9973
TS	−1	−0.0019 ± 00003	0.9986
BS	−1	−0.0018 ± 00004	0.9963
PYR	+	+0.0007 ± 00002	0.9987
NMA	+	+0.0007 ± 00002	0.9979

[a] Standard deviations based on five replicate injections of each sample.

elution band (not shown), which occurs between −100 and −200 mV, supports the transformation.

The slope of the plots in Fig. 2 correlates with analyte charge. The divalent anions exhibit the greatest changes, while the monovalent anions and cations undergo opposing and weaker dependencies. Furthermore, the cations are less sensitive to changes in E_{app} than the monovalent anions. This difference is ascribed to contributions by nonelectrostatic interactions between the analyte-stationary phase, i.e., the donor–accepter interactions between the π-systems of the aromatic analytes and the stationary phase, which act in concert with the electrostatic interactions for anions but in opposition for cations. This argument is founded on the retention of benzene and its monosubstituted analogs, which undergo a decrease as E_{app} moves negatively [5,40]. The slope of a $\ln k' - E_{app}$ plot for benzene, for example, equals $0.00035\,mV^{-1}$, a value that has the same order of magnitude as the cations in Table 1. Therefore, if the aromatic π-systems for the cations behave similarly, their dependencies on E_{app} would decrease by a comparative level. The counter argument applies to the retention dependence of aromatic anions. This claim is supported by the slight difference in the slope for 1,5-NDS and 1,3-BDS, which are divalent anions that have π-systems with different sizes. We add that the EMLC-based retention of inorganic monovalent anions [41] yield slopes that are roughly half those observed for aromatic monoanions when using a similar mobile phase (not shown), which also supports this conclusion.

Finally, the role of electrostatics is revealed by the $\ln k' - E_{app}$ curves for CBS, TS, and BS, which are indistinguishable from each other even though the absolute values of their retention differ. These results indicate that retention is manipulated largely by changes in electrostatic interactions rather than specific surface–analyte interactions. Although specific interactions (e.g., dispersive, hydrophobic, dipole-induced dipole, etc.) contribute to the magnitude of sorption, the similarities in the slopes between analytes of like charge argue that the EMLC-based changes in $\Delta G_{a\text{-lyte}}$ can be accounted for primarily by electrostatic arguments. The next two sections further investigate this possibility by examining the influence of supporting electrolyte identity and concentration on retention.

3.2. Effect of supporting electrolyte composition

Chromatograms for BDS and BS are given in Fig. 3 at +200 mV for five different monovalent supporting electrolytes ($NaPF_6$, $NaClO_4$, $NaBF_4$, NaOH, and NaF) with concentrations fixed at 0.1 M. As is apparent, the identity of the electrolyte anion has a strong impact on retention. These differences suggest that interactions of the supporting electrolyte with the stationary phase beyond electrostatics must be considered in the development of a retention mechanism.

In general, the eluotropic order in Fig. 3 agrees with expectations drawn from the specific adsorption of these anions onto carbon materials and solid electrodes in the sorption and electrosorption literature [42–47]. The differing degrees in the specific adsorption of the electrolyte anions are described by $\Delta G_{-e\text{-lyte}}$ and signify a competition between solute and electrolyte for sorption sites on the stationary phase. Thus, specific adsorption, which can involve solvophobic, dispersive, dipole induced dipole and charge transfer interactions between the anion and the electrode surface, must be accounted for in a model of retention in EMLC.

3.3. Effect of supporting electrolyte concentration

The influence of supporting electrolyte concentration on the separation of BS, TS, and CBS is shown in Fig. 4 at +200 mV using $LiClO_4$. The elution order (BS < TS < CBS) remained constant for all electrolyte concentrations, but

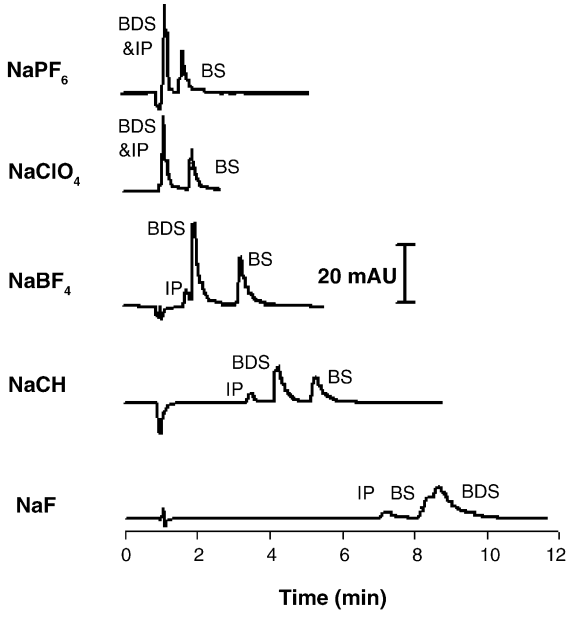

Fig. 3. Chromatograms illustrating the effect of supporting electrolyte identity on the retention of BS (8 μM) and BDS (14 μM) at E_{app} = +200 mV vs. Ag/AgCl sat'd NaCl. A third peak (IP) is present in each chromatogram which was determined to be a contaminant from the BDS starting material by evaluation of individual injections. The mobile phase consisted of 10% acetonitrile in water with the designated supporting electrolyte present at a concentration of 0.1 M. The flow rate is 0.4 mL/min.

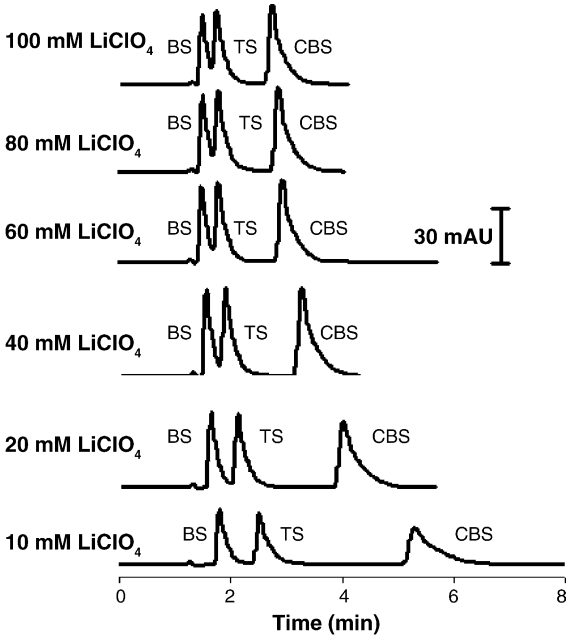

Fig. 4. Chromatograms illustrating the effect of supporting electrolyte concentration on the separation of BS (8 μM), TS (14 μM), and CBS (23 μM). An E_{app} of +200 mV vs. Ag/AgCl sat'd NaCl was employed. Mobile phase consisted of 10% acetonitrile in water with the indicated supporting electrolyte concentration. Flow rate is 0.4 mL/min.

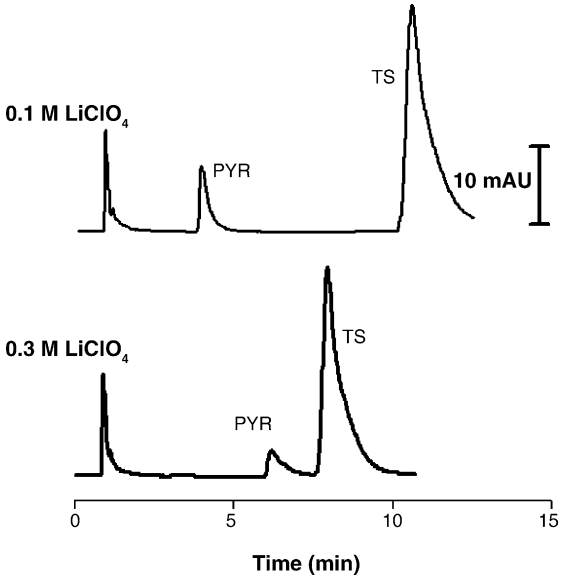

Fig. 5. Effect of supporting electrolyte concentration on the retention of oppositely charged TS (18 μM) and PYR (31 μM). The E_{app} was set to +400 mV vs. Ag/AgCl sat'd NaCl. The mobile phase consists of 10% acetonitrile in water with the indicated supporting electrolyte concentration; TFA was added to mobile phase to adjust the pH ∼ 3. The flow rate is 0.4 mL/min.

retention decreased with increasing electrolyte concentration. Relatively, the retention for each analyte decreased by ∼60% for a 10-fold increase in electrolyte concentration. This decrease, however, is much different than expected from purely electrostatic considerations. An electrostatic adsorption model predicts that a 10-fold increase in electrolyte concentration will reduce analyte retention to 10% of the initial value [48]. We attribute this discrepancy to differences in the specific adsorption of the analyte and the electrolyte, with the specific adsorption of the negatively charged analyte competing favorably with that of the electrolyte anion.

Literature reports place the potential of zero charge (PZC) of the stationary phase between −200 < PZC < +100 mV (versus Ag/AgCl saturated NaCl) [49,50]. Therefore, an interfacial excess of electrolyte anions exists under the conditions in Fig. 4, since the value of E_{app} is more positive than that expected for the PZC. The electrolyte anions would then compete with the negatively charged aromatic sulfonates in counterbalancing the positively charged surface, and a higher supporting electrolyte concentration would then shield analytes from the positively charged surface. As a consequence, the magnitude of the electrostatic attraction and therefore retention would decrease. Insights into the competition at the stationary phase, whether specifically for adsorption sites and/or indirectly through electrostatic interactions, may be determined by comparing the experimental data with models of the architecture of an electrified interface, and will be detailed shortly.

Fig. 5 shows that a change in supporting electrolyte concentration (0.1–0.3 M) has a contrasting effect on the retention of analytes with opposite charge. This difference reveals that a purely competitive adsorption mechanism is not the sole factor responsible for the change in retention. That is, the retention of PYR would also be expected to decrease because of the increase in the cation (Li^+) concentration in the mobile phase. The increase in retention for PYR, however, indicates that electrolyte concentration has a strong influence on the electrostatic field experienced by the analyte and may shield the analyte from the stationary phase. In other words, ion-pairing type interactions between solute and surface bound electrolyte anions, $\Delta G_{+N\text{-}N}$, may become more pronounced at higher electrolyte concentrations, which counters repulsion and increases PYR retention. Therefore, the basic model of how an electric field contributes to $\Delta G_{a\text{-}lyte}$ must be extended to include the influence of supporting electrolyte concentration.

The strong contrast in the behavior of the oppositely charged analytes in Fig. 5 can be reasonably explained by the Gouy–Chapman (G–C) theory for the structure of the electrical double layer [15,48]. Fig. 6 illustrates how a change in supporting electrolyte concentration influences the structure of an electrified interface at a positively charged electrode via G–C theory. As shown, G–C theory predicts that an increase in supporting electrolyte concentration will decrease the thickness of the diffuse region of the electrical double layer. Experiments have shown that the diffuse region effectively vanishes at supporting electrolyte concentrations greater than 0.1 M [51], which results in the accumulation of

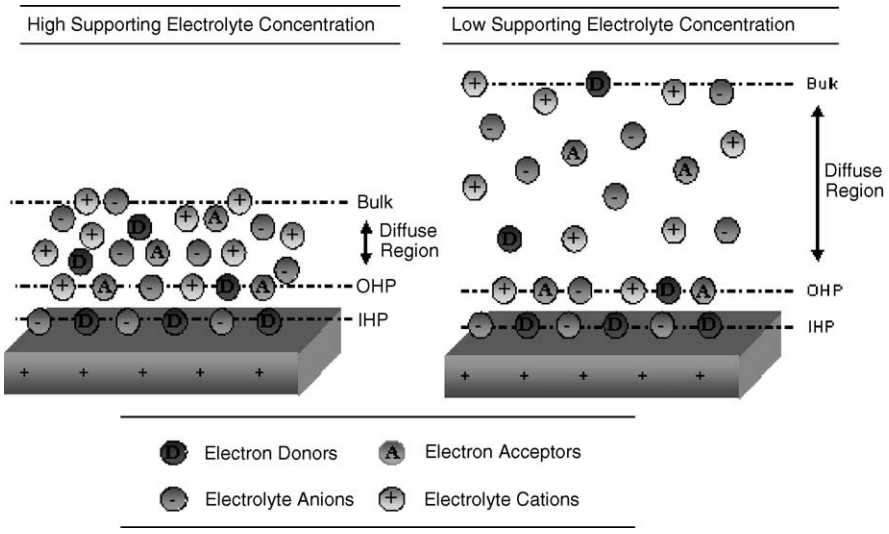

Fig. 6. Idealized depiction describing the influence of supporting electrolyte on the thickness of the electrical double layer at applied potentials positive of the PZC. These depiction omit contributions from the mobile phase solvent.

charge on the solution side of the liquid–solid interface solely at the inner Helmholtz (IHP) and the outer Helmholtz planes (OHP).

At higher supporting electrolyte concentrations, solutes in bulk solution are shielded from the electric field imposed by the potential applied to the stationary phase by the counter-ions held in both planes. Shielding reduces the extent of electrostatic interactions between the packing and charged analyte. As a consequence, an analyte at a given distance from the electrode surface would have a stronger electrostatic interaction with the stationary phase at lower supporting electrolyte concentrations. The next section examines these data within the context of a retention model.

3.4. Modeling EMLC

Together, these data indicate that $\Delta G_{\text{a-lyte}}$, $\Delta G_{\pm\text{e-lyte}}$, and $\Delta G_{\pm\text{N-N}}$ play a more prominent role in retention than $\Delta G_{\pm\text{int}}$. Since $\Delta G_{\pm\text{e-lyte}}$ changes with E_{app}, the competition for sorption sites is potential dependent and is the likely origin for the nonlinear behavior observed for some analytes in EMLC. Furthermore, $\Delta G_{\text{a-lyte}}$ can be dissected into electrostatic and non-electrostatic components in which the supporting electrolyte concentration can modulate electrostatics and the available number of sorption sites. The influence of supporting electrolyte concentration on electrostatics will be described first by classical G–C theory. The use of a Langmuir adsorption isotherm to describe the influence of electrolyte concentration on non-electrostatic components (i.e., specific adsorption of electrolyte) will then ensue through comparisons to analyses from models for ion-paring chromatography (IPC).

The relationship between the charge on the electrode surface, applied potential, and supporting electrolyte concentration in the GC theory for a 1:1 supporting electrolyte is given by [15,52]

$$q_{\pm\text{sol}} = \sqrt{\frac{\varepsilon C_{\text{M}} kT}{2\pi}}\left(\text{e}^{-z_{\pm}e_0\Psi/2kT} - 1\right) \tag{1}$$

where $q_{\pm\text{sol}}$ is the excess interfacial charge on the solution side of the interface, ε the dielectric constant of solvent in the interphase, C_{M} the bulk concentration of supporting electrolyte, k the Boltzmann constant, T the temperature in Kelvin, z_i the valence of species i, e_0 the electronic charge, and Ψ is the surface potential. The modification of Eq. (1) to describe k' as a function of potential and concentration of supporting electrolyte is presented in Appendix A; the result is given by Eq. (2), where A is the surface area of the stationary phase, V_{M} the volume of the mobile phase, and the Debye length, κ^{-1}, is defined in Eq. (3). The other terms have the same meaning as before.

$$k' = \frac{A}{V_{\text{M}}\kappa}\left(\text{e}^{-ze_0\Psi/kt} - 1\right) + 1 \tag{2}$$

$$\kappa^{-1} = \left(\frac{\varepsilon kT}{2\pi(zF)^2 C_{\text{M}}}\right)^{1/2} \tag{3}$$

Eq. (2) predicts that the magnitude of k' is inversely dependent on $\sqrt{C_{\text{M}}}$ while the trends induced by changing electrolyte concentration depend on analyte charge and E_{app}. That is, the value for the parenthetical term in Eq. (2) is less than zero for a cation at $E_{\text{app}} \gg \text{PZC}$, triggering an increase in k' with increasing electrolyte concentration. In contrast, the term in parenthesis is positive for an anion and k' would decrease as C_{M} increases.

The influence of E_{app} on the relationship between k' and C_{M} is provided for three aromatic sulfonates in Fig. 7. Importantly, k' for all analytes becomes less sensitive to changes in supporting electrolyte concentration as the value of E_{app}

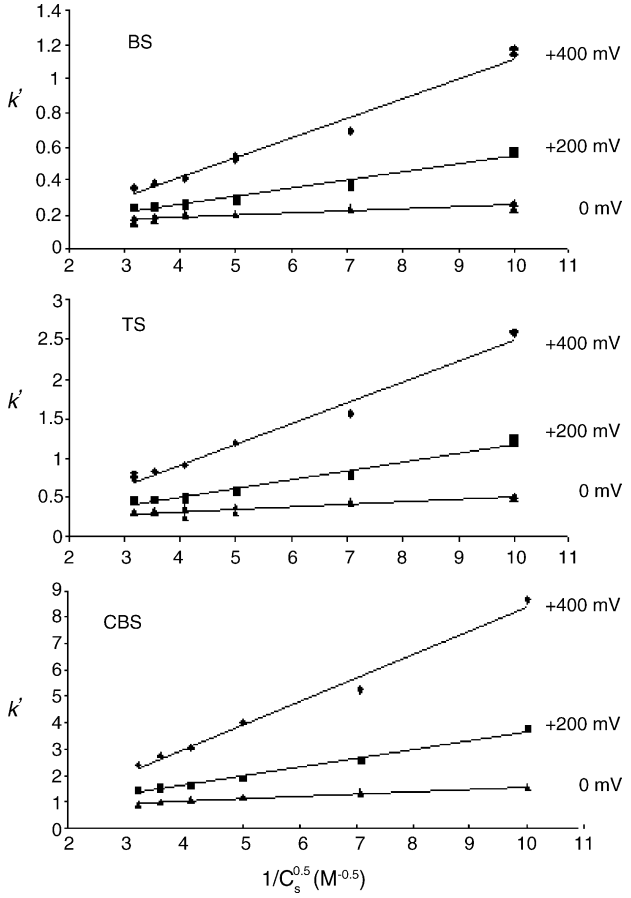

Fig. 7. A plot of k' vs. $1/\sqrt{F^-}$ for BS (8 μM), TS (14 μM), and CBS (23 μM). Three replicate injections were made at each concentration studied, and the data points are roughly the size of the error bars. The mobile phase consisted of 10% acetonitrile in water using sodium fluoride as the supporting electrolyte at concentrations of 0.01, 0.02, 0.04, 0.06, 0.08 and 0.1 M.

approaches the PZC by becoming more negative. In this case, the parenthetical term in Eq. (2) moves closer to zero, which suggests that analyte retention becomes independent of supporting electrolyte concentration and that the electrostatic component of retention has no influence at the PZC. These findings reinforce the notion that retention would be governed only by specific interactions with the surface at the PZC.

G–C theory has been applied extensively in mechanistic investigations of IPC [28,31]. There are two prevailing developments: the Stahlberg [30] and Cantwell [29] models. Both employ the key assumptions of G–C theory, which are equally applicable to EMLC. In IPC, the charge density of the packing, $\sigma_{\pm}$, is determined by the concentration of charged groups attached to the stationary phase and by the concentration of the pairing ion. In EMLC, $\sigma_{\pm}$, stems from the potential applied to the polarizable stationary–mobile phase interface. Both IPC models invoke G–C theory to describe the electrostatic interactions of relevance, but differ in how the direct competition for sorption sites occurs. The Stahlberg model anticipates a linear plot of $\log k'$ versus $\log C_s$ by contact adsorption of electrolyte in a modified Langmuir adsorption isotherm. The Cantwell model, on the other hand, predicts an inverse relationship between k' and electrolyte concentration due to competition for adsorption sites.

To ascertain which model is best suited for interpreting EMLC data, R^2 values from a regression analysis for plots of k' versus $1/C_s$ given by Cantwell, $\log k'$ versus $\log C_s$ as modeled by Stahlberg, and k' versus $1/\sqrt{C_s}$ relationship represented by Eq. (2) (EDL) are provided in Table 2. While mathematically similar, the Stahlberg model only differs from Eq. (2) through an additional term that employs a potential dependent Langmuir adsorption isotherm to describe the extent of contact adsorption. As mentioned, the changes in the slope at different values of E_{app} for each type of plot can be predicted by double layer theory. Moreover, Table 2 suggests that the reliability of these models to describe EMLC retention is potential dependant. For example, when sodium fluoride is the supporting electrolyte, these models appear less effective at −50 mV with respect to the other values of E_{app}. Lithium perchlorate shows a similar deficiency at −300 mV.

The utility of these models to predict the retention dependence on electrolyte concentration is consistent with expectations. That is, the contribution of electrostatic and ion-exchange processes to retention is at a minimum at the PZC. Thus, the key contributor to retention would be different at the PZC than at potentials removed from the PZC. Furthermore, retention at the PZC should at least qualitatively correlate with reversed phase behavior, which is consistent with the observed hydrophobic contribution to retention observed at carbonaceous stationary phases [25].

Table 2 also argues that all three mechanisms reasonably describe the dependence of analyte retention on E_{app} at values removed from the PZC, although the Stahlberg and the EDL models show the strongest correlations. The lower correlation with the Cantwell model argues that an ion-exchange process in the diffuse region is not central in determining retention in EMLC. While possibly a coincidence, Table 2 suggests that, on average, the EDL model is somewhat more predictive with NaF as the supporting electrolyte, whereas the Stahlberg model is a little more reliable when $LiClO_4$ is used.

Fluoride is typically viewed as a weak specific adsorbent on electrodes, which suggests that the predominant competition between fluoride and the analyte occurs in the electrical double layer. Experiments using perchlorate correlate better with Stahlberg's model, which points to a competition for adsorption sites and is consistent with perchlorate being a stronger eluent than fluoride. Taken together, these results signify a variable retention mechanism that can be modeled by ion-exchange processes at more extreme potentials and by reverse phase processes near the PZC.

3.5. Use of supporting electrolyte in EMLC

Finally, Fig. 8 shows how the supporting electrolyte concentration can be used to manipulate EMLC separations. Chromatogram 8A is the isocratic separation of a mixture of BS, TS, NMA, and CBS with 0.1 M $LiClO_4$ used as the

Table 2
Correlation analysis of ion-exchange models with experimental data

Analyte	E_{app} (mV)	Cantwell (Naf)	Stahlberg (Naf)	EDL (Naf)	Cantwell ($LiClO_2$)	Stahberg ($LiClO_2$)	EDL ($LiClO_2$)
TS	+50	0.9846	0.9980	0.9985	–	–	–
TS	0	0.9623	0.9803	0.9979	0.9514	0.9567	0.9628
TS	−50	0.7408	0.7826	0.7685	0.9538	0.9128	0.9560
TS	−100	0.9627	0.9990	0.9881	0.9542	0.9215	0.9557
TS	−150	0.9863	0.9872	0.9973	0.9160	0.9617	0.9586
TS	−200	–	–	–	0.9440	0.8813	0.9514
TS	−300	–	–	–	0.6748	0.8675	0.8884
TS	−400	–	–	–	0.9490	0.9358	0.9154
	Average	0.9273	0.9494	0.9501	0.9062	0.9204	0.9412
BS	+50	0.9551	0.9970	0.9836	–	–	–
BS	0	0.9584	0.9969	0.9851	0.9371	0.9610	0.9560
BS	−50	0.6602	0.6958	0.7093	0.9605	0.9354	0.9552
BS	−100	0.9680	0.9958	0.9891	0.8776	0.9477	0.9186
BS	−150	0.9744	0.9974	0.9943	0.8849	0.9416	0.8925
BS	−200	–	–	–	0.9121	0.9275	0.9018
BS	−300	–	–	–	0.6143	0.7431	0.7675
BS	−400	–	–	–	0.8654	0.9505	0.9696
	Average	0.9032	0.9366	0.9323	0.8646	0.9153	0.9087
CBS	+50	0.9431	0.0.9906	0.9746	–	–	–
CBS	0	0.9759	0.9982	0.9946	0.9477	0.9645	0.9628
CBS	−50	0.9227	0.9735	0.9440	0.9682	0.9349	0.9560
CBS	−100	0.9858	0.9899	0.9975	0.9442	0.9504	0.9357
CBS	−150	0.9600	0.9984	0.9859	0.9666	0.9254	0.9301
CBS	−200	–	–	–	0.9597	0.9448	0.9386
CBS	−300	–	–	–	0.7068	0.8244	0.7984
CBS	−400	–	–	–	0.8769	0.8499	0.8234
	Average	0.9575	0.9901	0.9793	0.9100	0.9135	0.9064
1.3-BDS	+50	0.9574	0.9626	0.9674	–	–	–
1.3-BDS	0	0.9190	0.9700	0.9550	0.9330	0.9671	0.9578
1.3-BDS	−50	0.6694	0.6091	0.6983	0.8739	0.9371	0.9156
1.3-BDS	−100	0.8742	0.9650	0.9209	0.8985	0.9468	0.9318
1.3-BDS	−150	0.7895	0.9252	0.9245	0.8968	0.9531	0.9343
1.3-BDS	−200	–	–	–	0.9658	0.9547	0.9043
1.3-BDS	−300	–	–	–	0.7058	0.7750	0.7423
1.3-BDS	−400	–	–	–	0.9210	0.9389	0.9366
	Average	0.8419	0.8864	0.8992	0.8850	0.9247	0.9032
15-HDS	+50	0.8962	0.9690	0.9742	–	–	–
15-HDS	0	0.9616	0.9511	0.9627	0.9550	0.9695	0.9576
15-HDS	−50	0.5843	0.6134	0.6785	0.9679	0.9359	0.9484
15-HDS	−100	0.9720	0.9912	0.9904	0.7460	0.9301	0.8908
15-HDS	−150	0.8542	0.9532	0.9906	0.8936	0.8922	0.9257
15-HDS	−200	–	–	–	0.9190	0.8828	0.8764
15-HDS	−300	–	–	–	0.7071	0.7949	0.7689
15-NDS	−400	–	–	–	0.9355	0.9306	0.9279
	Average	0.8537	0.8956	0.9193	0.8749	0.8909	0.8994
	Total average	0.8967	0.9316	0.9360	0.8881	0.9129	0.9118

R^2 values taken from plots of k' vs. $1/C$ (Cantwell), $\log k'$ vs. $\log C$ (Stahlberg), and k' vs. $C^{-1/2}$ (EDL). Plots generated from chromatographic separations performed on a mixture of aromatic sulfonates at multiple concentrations of NaF or $LiClO_4$ for each value of E_{app}. Each entry is the average of five replicate injections. Cantwell average: 0.8924, Stahlrerg average: 0 9223, EDL average: 0 9239.

supporting electrolyte. Under these conditions, baseline resolution of BS and CBS was obtained, but the oppositely charged TS and NMA co-eluted. The results reported in the preceding sections suggest two possible ways to resolve the co-eluents: a change in E_{app} (Fig. 2) or a change in supporting electrolyte concentration (Figs. 4 and 5). The application of a concentration gradient would be particularly attractive when the electroactivity of one or more of the components in a sample would possibly preclude the use of a change in E_{app} to fine-tune the separation.

In an effort to resolve TS and NMA by changing the supporting electrolyte concentration, two stepwise gradients in

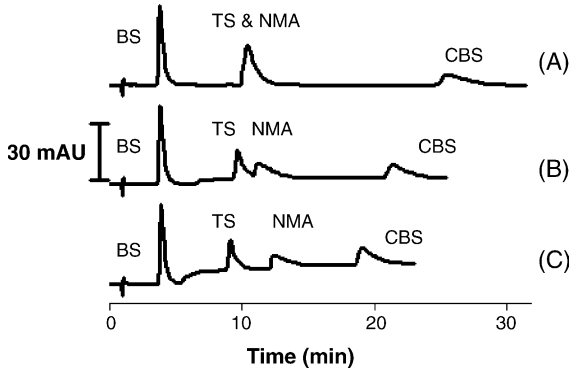

Fig. 8. Chromatograms that illustrate the utility of a supporting electrolyte concentration gradient for the enhancement of EMLC separations. The sample mixture was composed of BS (8 μM), TS (14 μM), CBS (23 μM), and NMA (22 μM). The mobile phase consisted of 5% acetonitrile in water with TFA added to adjust the solution pH to ∼2. The absorbance at 212 nm was monitored. The flow rate was set at 0.4 mL/min. The applied potential is +400 mV vs. Ag/AgCl sat'd NaCl.

Table 3
The supporting electrolyte concentration gradient used to generate the corresponding chromatograms in Fig. 8

Time (min)	0–5	5–13	18–
A	0.1 M $LiClO_4$	0.1 M $LiCl0_4$	0.1 M $LiClO_4$
B	0.1 M $LiClO_4$	0.2 M $LiCl0_4$	0.2 M $LiClC_4$
C	0.1 M $LiClO_4$	o.3 M $LiClo_4$	0.4 M $LiClC_4$

$LiClO_4$ concentration were tested. These results are given by chromatograms 8B and 8C; the mobile phases are detailed in Table 3. The changes in the baseline observed in both chromatograms are due to the increase in electrolyte concentration, reflecting the absorption of perchlorate ion at 212 nm. Partial resolution of TS and NMA was obtained when the electrolyte concentration was increased (chromatogram 8B). Baseline resolution was achieved using the larger stepwise concentration gradient (chromatogram 8C). These results show that changes in the electrolyte concentration alter the EMLC selectivity, and are consistent with the discussions based on the data in Figs. 2–7. Fig. 8 also demonstrates that altering the concentration of electrolyte can be used to optimize the analysis time. The retention CBS was decreased by ∼10 min in moving from the isocratic separation in chromatogram 8A to the stepwise electrolyte concentration gradient in chromatogram 8C.

4. Conclusion

This paper examined the influence of supporting electrolyte on the retention of charged analyte molecules in EMLC. Both direct and indirect competition for adsorption sites onto the stationary phase surface strongly affected retention. Direct competition for occupancy of sorption sites on the stationary phase is expressed as a combination of $\Delta G_{\pm\text{e-lyte}} + \Delta G_{\pm\text{N-N}}$, which influence retention most strongly with changes in the identity of the electrolyte. The inclusion of direct competition into the retention mechanism for EMLC to describe changes in electrolyte identity requires information about the total free energy of adsorption for the electrolyte itself. Indirect competition may be explained as a modulation of the electrostatic potential profile component of $\Delta G_{\text{a-lyte}}$, and was found to be a significant factor towards changes in analyte retention as a function of electrolyte concentration. Furthermore, the influence of electrolyte concentration was found to depend on analyte charge and E_{app}. This behavior can be explained by a shielding of electrostatic analyte-stationary phase interactions via a change in the potential profile as a function of distance from the electrode surface, as calculated from electrical double layer theory. Furthermore, the use of Gouy–Chapman–Stern diffuse double layer in future experiments may prove valuable in determining fundamental electrochemical properties of the stationary–mobile phase interface in EMLC such as the PZC and electrical capacitance of our columns.

Acknowledgements

Discussions with D. Weisshaar are greatly appreciated. D.W.K. gratefully acknowledges the assistance of a Phillips Graduate Research Fellowship. This work was supported by the Office of Basic Energy Science of the US Department of Energy. The Ames Laboratory is operated for the US Department of Energy by Iowa State University under Contract No. W-7405-eng-82.

Appendix A

The relationship between charge in solution, E_{app}, and distance from the electrode surface for a 1:1 supporting electrolyte according to Gouy–Chapman theory was given by Eq. (1). When E_{app} is negative of the PZC, Eq. (1) yields the value of $q_{+\text{sol}}$, while at positive potentials versus the PZC Eq. (1) provides the value for $q_{-\text{sol}}$. The charge in solution at the electrified interface is directly related to the surface excess of ions through the following relationship:

$$q_{\pm} = zF\Gamma_{\pm} \tag{A.1}$$

where $\Gamma_{\pm}$ is the surface excess of either the cations (+) or anions (−) at the electrified interface. For the situation when the applied potential is positive of the PZC, Eq. (A.1) can be inserted into Eq. (1) to give:

$$zF\Gamma_{-} = \sqrt{\frac{\varepsilon C_{\text{M}} kT}{2\pi}}(\text{e}^{-z_{-}e_0\Psi_0/2kT} - 1) \tag{A.2}$$

The surface excess describes adsorption of a given ion at the interface, and is related to the retention factor (k') that is determined chromatographically. In other words, Γ describes the difference between the amount of a given species at the

interface, n_s, and that in the bulk solution, n_M, after normalization for the area of the interface. Eq. (A.3) presents the formal definition of Γ_-.On the other hand, k' describes the ratio of absolute amounts of a species adsorbed on the stationary phase and in the mobile phase as shown in Eq. (A.4).

$$\Gamma_- = \frac{1}{A}(n_S - n_M) \tag{A.3}$$

$$k' = \frac{C_S V_S}{C_M V_M} = \frac{n_S}{n_M} \tag{A.4}$$

where C_S and C_M are the surface and bulk solution concentrations, respectively, and V_S and V_M are the stationary phase and mobile phase volumes, respectively. By substitution $n_M k'$ in Eq. (A.4) for n_S in Eq. (A.3), the relationship between retention factor and surface excess can be determined:

$$\Gamma_- = \frac{n_M}{A}(k' - 1) \tag{A.5}$$

Substitution of Eq. (A.5) into Eq. (A.2) shows the relationship between k' and potential at the interface as modified by supporting electrolyte concentration:

$$\frac{zFn_M}{A}(k' - 1) = \sqrt{\frac{\varepsilon C_M kT}{2\pi}}(e^{-z_- e_0 \Psi_0/2kT} - 1) \tag{A.6}$$

Rearrangement of A.6 and using the relationship of $n_M = C_M V_M$ gives:

$$(k' - 1) = \frac{A}{V_M}\sqrt{\frac{\varepsilon kT}{2\pi(zF)^2 C_M}}(e^{-z_- e_0 \Psi_0/2kT} - 1) \tag{A.7}$$

The square root term in Eq. (A.7) is the Debye length, κ^{-1}, which characterizes the distance between two plates of a parallel plate capacitor that would mimic the real situation occuring in solution. Substitution of κ^{-1} into Eq. (A.7) and adding one to both sides then gives Eq. (2), which was presented in an earlier section. This relationship describes the influence of potential and supporting electrolyte concentration on the retention factor of an ionic species based solely on electrostatic interactions.

References

[1] J.A. Harnisch, M.D. Porter, Analyst 126 (2001) 1841.
[2] M.D. Porter, H. Takano, in: I.D. Wilson, E.R. Adlar, M. Cooke, C.F. Poole (Eds.), Encyclopedia of Separation Science, Academic Press, London, 2000, p. 636.
[3] E.-Y. Ting, M.D. Porter, Anal. Chem. 70 (1998) 94.
[4] R.S. Deinhammer, E.-Y. Ting, M.D. Porter, J. Electroanal. Chem. 362 (1993) 295.
[5] R.S. Deinhammer, E.-Y. Ting, M.D. Porter, Anal. Chem. 67 (1995) 237.
[6] R.S. Deinhammer, M.D. Porter, K. Shimazu, J. Electroanal. Chem. 387 (1995) 35.
[7] H. Deng, G.J.V. Berkel, H. Takano, D. Gazda, M.D. Porter, Anal. Chem. 72 (2000) 2641.
[8] E.-Y. Ting, M.D. Porter, J. Chromatogr. A 793 (1998) 204.
[9] E.-Y. Ting, M.D. Porter, Anal. Chem. 69 (1997) 675.
[10] S. Wang, M.D. Porter, J. Chromatogr. A 828 (1998) 157.
[11] M. Ho, S. Wang, M.D. Porter, Anal. Chem. 70 (1998) 4314.
[12] M.W. Knizia, K. Vuorilehto, J. Schrader, D. Sell, Electroanalysis 15 (2003) 49.
[13] M. Shibukawa, A. Unno, T. Miura, A. Nagoya, K. Oguma, Anal. Chem. 75 (2003) 2775.
[14] L.M. Ponton, M.D. Porter, Anal. Chem. 76 (2004) 5823.
[15] J.O.M. Bockris, A.K.N. Reddy, Modern Electrochemistry: An Introduction to an Interdisciplinary Area, Plenum Press, New York, 1970.
[16] J.A. Harnisch, D.B. Gazda, J.W. Anderegg, M.D. Porter, Anal. Chem. 73 (2001) 3954.
[17] P. Nikitas, J. Electroanal. Chem. 484 (2000) 137.
[18] M. Shibukawa, H. Terashima, H. Nakajima, K. Saitoh, Analyst 129 (2004) 623.
[19] M. Shibukawa, A. Unno, y. Oyashiki, T. Miura, A. Nagoya, K. Oguma, Anal. Commun. 34 (1997) 397.
[20] A. Tornkvist, K.E. Markides, L. Nyholm, Analyst 128 (2003) 844.
[21] M. Balcan, T. Cserhati, E. Forgacs, Anal. Lett. 30 (1997) 883.
[22] V. Coquart, M.-C. Hennion, J. Chromatogr. 600 (1992) 195.
[23] M.-C. Hennion, V. Cocquart, J. Chromatogr. 642 (1993) 211.
[24] N. Tanaka, T. Tanigawa, K. Kimata, K. Hosoya, T. Araki, J. Chromatogr. 549 (1991) 29.
[25] P. Ross, LC/GC 18 (2000) 14.
[26] J.H. Knox, P. Ross, in: P.R. Brown, E. Grushka (Eds.), Advances in Chromatography, Marcel Dekker, New York, 1997, p. 73.
[27] L.M. Ponton, M.D. Porter, D.W. Keller, in preparation.
[28] F.F. Cantwell, L.L. Glavina, J.-G. Chen, S.G. Weber, J. Chromatogr. A 656 (1993) 549.
[29] F.F. Cantwell, S. Puon, Anal. Chem. 51 (1979) 623.
[30] J. Stahlberg, Anal. Chem. 66 (1994) 440.
[31] J. Stahlberg, J. Chromatogr. A 855 (1999) 3.
[32] J.H. Knox, B. Kaur, J. Chromatogr. 352 (1986) 3.
[33] P. Ross, J.H. Knox, in: P.R. Brown, E. Grushka (Eds.), Advances in Chromatography, Marcel Dekker Inc., New York, 1997, p. 121.
[34] A.E. Martell, R.M. Smith, Critical Stability Constants Amines, Plenum Press, New York, 1975.
[35] Hewlett-Packard, in: Understanding Your Chemstation, Hewlett-Packard, Wilmington, 1994, p. 185.
[36] H.M. McNair, W.M. Cook, Am. Lab. 5 (1973) 12.
[37] E. Grushka, M.N. Myers, P.D. Schettler, J.C. Giddings, Anal. Chem. 41 (1969) 889.
[38] H. Takano, M.D. Porter, Proc. Electrochem. Soc. 99–105 (1999) 50.
[39] H. Lund, O. Hammerich, Organic Electrochemistry, fourth edition, revised and expanded, Marcel Dekker, New York 2001.
[40] E.-Y. Ting, M.D. Porter, J. Electroanal. Chem. 443 (1998) 180.
[41] L.M. Ponton, M.D. Porter, J. Chromatogr. A. 1059 (2004) 103.
[42] W. Paik, M.A. Genshaw, J.O.M. Bockris, J. Phys. Chem. 74 (1970) 4266.
[43] J.S. Mattson, H.B. Mark, Activated Carbon: Surface Chemistry and Adsorption from Solution, Marcel Dekker, New York, 1971.
[44] D.D. Bode, T.N. Andersen, H. Eyring, J. Phys. Chem. 71 (1967) 792.
[45] R.S. Perkins, T.N. Andersen, in: J.O.M. Bockris, B.E. Conway (Eds.), Modern Aspects of Electrochemistry, Plenum Press, New York, 1969, p. 203.
[46] C. Elkafir, P. Chaimbault, M. Dreux, J. Chromatogr. A 829 (1998) 193.
[47] B.E. Conway, Electrochim. Acta 40 (1995) 1501.
[48] J.O.M. Bockris, A.K.N. Reddy, Modern Electrochemistry, An Introduction to An Interdisciplinary Area, vol. 2, Macdonald, London, 1970.
[49] J.-P. Randin, in: A.J. Bard (Ed.), Encyclopedia of Electrochemistry of the Elements, Marcel Dekker, New York, 1976, p. 2.
[50] K. Kinoshita, Carbon Electrochemical and Physicochemical Properties, Wiley, New York, 1988.
[51] D.C. Grahame, Chem. Rev. 41 (1947) 441.
[52] P. Delahay, Double Layer and Electrode Kinetics, Interscience, New York, 1965.